

Free vibrations of arbitrary quadrilateral thick plates with internal columns and uniform elastic edge supports by pb-2 Ritz method

L.H. Wu*

Department of Engineering Mechanics, Shijiazhuang Tiedao University, Shijiazhuang 050043, P.R. China

(Received March 30, 2012, Revised September 13, 2012, Accepted September 26, 2012)

Abstract. Free vibration analysis of arbitrary quadrilateral thick plates with internal columns and elastic edge supports is presented by using the powerful pb-2 Ritz method and Reddy's third order shear deformation plate theory. The computing domain of arbitrary quadrilateral planform is mapped onto a standard square form by coordinate transformation. The versatile pb-2 Ritz functions defined by the product of a two-dimensional polynomial and a basic function are taken to be the admissible functions. Substituting these displacement functions into the energy functional and minimizing the total energy by differentiation, leads to a typical eigenvalue problem, which is solved by a standard eigenvalue solver. Stiffness and mass matrices are numerically integrated over the plate by using Gaussian quadrature. The accuracy and efficiency of the proposed method are demonstrated through several numerical examples by comparison and convergence studies. A lot of numerical results for reasonable natural frequency parameters of quadrilateral plates with different combinations of elastic boundary conditions and column supports at any locations are presented, which can be used as a benchmark for future studies in this area.

Keywords: free vibration; thick plate; arbitrary quadrilateral plate; third order shear deformation theory; pb-2 Ritz method; coordinate transformation

1. Introduction

Plates having internal column supports are typical structures in civil engineering. The internal columns can greatly enhance the loading capacity and improve the dynamic characteristics of the plate. Usually the plate is modeled to be fully clamped or simply supported along four edges for simplification of analysis. However, such models are not completely in accordance with the actual situation. The edges of the plates are restrained much more like elastic restraints. Therefore, it is important for designers to understand how the columns and elastic springs affect the dynamic behaviors of these structures.

There are several models to describe the effect of a column on the vibration of a plate. The simplest model is to consider the column as a pinned point rigid support, which neglects the bending stiffness of the column in two transverse directions and takes the stiffness of column in longitudinal direction as infinity. An improved model is taking the column as three massless springs

*Corresponding author, Professor, E-mail: wulanhe@stdu.edu.cn

in the longitudinal and two rotational directions, which considered the effects of the column in three directions simultaneously.

Large amount of literature for free vibration studies of plates with either rigid or elastic point supports and elastic edge supports is available and here mentioned a little. Narita (1981, 1984, 1985) presented a series solution for the vibration analysis of rectangular plates with complex mixed conditions, point supports and cantilever plates with point constraints. A general study to vibration characteristics of rectangular plate with arbitrarily located point supports came from Fan and Cheung (1984) using the spline finite strip method. Cheung and Zhou (2000) presented a study on the vibrations of rectangular plates with elastic intermediate line-supports and edge constraints. Gorman (1999) gave an accurate solution for free vibration problems of point supported Mindlin plates by the superposition method. Kim and Dickinson (1987) used the Lagrangian multiplier method combined with the orthogonally generated polynomials to study the rectangular plates with point supports. Taking Timoshenko beam functions as admissible functions, Zhou (2001) investigated the free vibration problem of rectangular Mindlin plates with elastic supported edges using Rayleigh-Ritz method. Zhou and his partner Cheung (2002, 1999) used static beam functions as admissible functions to study the tapered rectangular plates with point supports and composite rectangular plates with point supports, respectively. They also studied the free vibration of thick laminated rectangular plates with point supports by finite layered method (Zhou *et al.* 2000). Recently, Zhou and his partners (2002, 2005, 2006) presented several papers to study the vibration problems of rectangular plate and skew plate with various boundary conditions using the Chebyshev polynomial and Ritz method based on the three dimensional theory. Lee and Lee (1997) studied the flexural vibration of rectangular plates on elastic point supports and discussed the effect of support stiffness. Huang and Thambiratnam (2001) studied the free vibrations of rectangular plates on elastic intermediate supports by the finite strip method. In their studies, four column models were employed and the effects of various factors on the natural frequencies were discussed in detail. Ohya *et al.* (2006) are the pioneers to analyze the vibration problem of plates with both elastic edge supports and internal column supports. They obtained an analytical solution for this problem via the superposition technique based on the first order shear deformation theory. Zhou and Ji (2006) proposed a direct method to derive the exact solution for the free vibration of thin rectangular plate with two opposite edges simply supported and with internal column supports. Recently, Wu and Lu (2011) presented a free vibration study of rectangular plates with internal columns and uniform elastic edge supports by pb-2 Ritz method. Wang *et al.* (2010) used the meshless method to study the transverse vibration of rectangular thin plate with finite elastic point support. The effects of rigid constant and locations of elastic point supports on the transverse vibration characteristics of thin plate are discussed in detail. Du and *et al.* (2011) presented an analytical method for determining the vibrations of two plates which are generally supported along the boundary edges and elastically coupled together at an arbitrary angle. Through solving the governing differential equations of plate, Seyedemad (2011) gave a closed form solution to the free vibration problem of thin rectangular plates on Winkler and Pasternak elastic foundation model which is distributed over a particular arbitrary area of the plate. Malekzadeh (2008) investigated the large amplitude free vibration of tapered rectangular thin plates with edges elastically restrained against rotations based on the thin plate theory in conjunction with von Karman assumption.

From the literature survey, one can easily find that most of the previous papers confined their studies to the vibration characteristics of rectangular plates. Few of them are concerned with the plates having arbitrary geometric shapes. Kanrunasena *et al.* (1996) presented the pioneer study to

vibration problems of plate with quadrilateral planforms, in which the powerful pb-2 Ritz method combined with the first order shear deformation theory were used. Wu (2001) investigated the free vibration of arbitrary quadrilateral plate by the weighted residual spline least squares method. Wu and his colleagues (2005) also presented the free vibrations of arbitrarily shaped thick plates by differential cubature method. In their studies, moderately thick plates with various geometric shapes such as rectangular, circular, quadrilateral, triangular, and super elliptical were all discussed. For plates with arbitrary shapes including internal column supports, Liew *et al.* (1994) investigated the vibration problems of Mindlin plates of arbitrary shapes with internal point supports by the Rayleigh Ritz method. Using A hybrid numerical approach combining the Rayleigh-Ritz method and the Lagrange multiplier method, Kitipornchai and *et al.* (1994) presented the free vibration study on Mindlin plates with arbitrary shapes and supported at corners. To the author's knowledge, no studies have been reported on the free vibration problem of arbitrary quadrilateral thick plate having internal columns together with elastic boundary conditions up to now. This is the motivation for this paper.

In the present paper, the powerful solution technique, pb-2 Ritz method combined with Reddy's higher order shear deformation plate theory are employed to treat the free vibration problem of quadrilateral thick plate with arbitrarily located internal columns and elastic boundary constrains in three directions. Two models of column are examined in this paper, one is taking it as three elastic massless springs in longitudinal and two rotational directions; the other is taking it as local uniformly distributed elastic springs only in the longitudinal direction. The correctness and numerical accuracy of the present method is verified firstly by the comparison of the present results with corresponding exact solutions or other numerical solutions in the open literature. Then parametric studies are conducted to examine the effects of the locations, sizes of the columns and different column models as well as the edge elastic support stiffness on the dynamic behavior of the plate column system.

2. Theoretical analysis

2.1 Displacement field

Consider an arbitrary quadrilateral plate shown in Fig. 1. The length of the edge AB, BC, CD are, respectively, a , b and c . The thickness of the plate is h . It is assumed that the plate is supported elastically in each direction at all edges of the plate, and with several columns in the plate domain. According to Reddy's third order shear deformation theory, the displacement field is as assumed as follows (Reddy 1999, Shufrin 2005)

$$\bar{u}(x, y, z) = u(x, y) + z\theta_x(x, y) - \frac{4z^3}{3h^2} \left[\theta_x(x, y) + \frac{\partial w}{\partial x} \right]$$

$$\bar{v}(x, y, z) = v(x, y) + z\theta_y(x, y) - \frac{4z^3}{3h^2} \left[\theta_y(x, y) + \frac{\partial w}{\partial y} \right]$$

$$\bar{w}(x, y, z) = w(x, y) \tag{1}$$

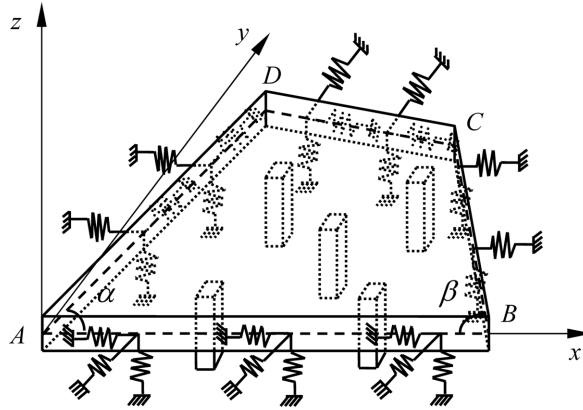
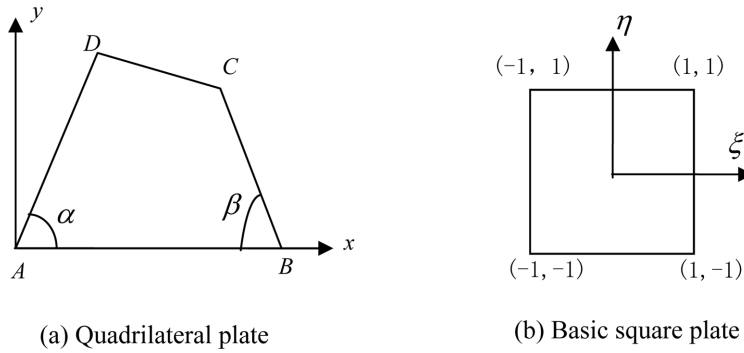


Fig. 1 The sketch of a quadrilateral plate with internal columns and elastic edge supports



(a) Quadrilateral plate (b) Basic square plate

Fig. 2 Coordinate transformation and geometric mapping

where \bar{u}, \bar{v} and \bar{w} are the displacement components along the x, y, z directions, respectively, at any point x, y, z of the plate thickness; $u(x, y)$ and $v(x, y)$ denote the in-plane displacements of the mid-plane respectively, in x and y direction, and $w(x, y)$ is the transverse deflection in the middle plane which assumed to be independent to z ; θ_x, θ_y are rotations of the plate normal about the y and x axes respectively. For isotropic materials, the in-plane displacements $u(x, y)$ and $v(x, y)$ can be neglected because there exists no coupling between in-plane and out of plane displacements.

2.2 Energy functional

The energy functional Π for plate vibration problem can be written in terms of the maximum strain energy U_{\max} and the maximum kinetic energy T_{\max} of the plate column system as

$$\Pi = U_{\max} - T_{\max} \tag{2}$$

where

$$U_{\max} = U^p + U^s + U^c \tag{3}$$

in which U^p, U^s and U^c are respectively, the strain energy of plate, springs at the edge of the plate

Table 1 Convergence and comparison of frequency parameters $\lambda = \omega a^2 \sqrt{\rho h/D}$ for a quadrilateral plate with different boundary conditions along four edges

Boundary Conditions	h/a	p	Mode sequence number						
			1	2	3	4	5	6	
CCCC	0.001	4	73.675	1932.623	1970.820	2792.888	4744.910	5208.290	
		6	67.847	132.839	144.283	229.367	265.399	279.189	
		8	67.397	130.100	141.779	207.769	226.618	256.193	
		9	67.384	129.704	141.583	206.199	222.824	254.757	
		10	67.381	129.609	141.545	205.674	221.282	254.070	
		Wu (2005)	67.378	129.585	141.527	205.596	226.666	—	
	0.2	4	42.345	68.232	72.306	95.891	102.678	109.840	
		6	42.317	67.987	72.120	94.432	99.145	108.114	
		8	42.315	67.979	72.115	94.341	98.875	108.026	
		9	42.315	67.978	72.115	94.337	98.868	108.023	
		10	42.315	67.978	72.114	94.337	98.867	108.022	
		Wu (2005)	42.311	67.982	72.134	94.347	98.983	—	
	SSSS	0.001	4	42.098	123.384	288.812	8 376.377	10999.847	11988.630
			6	36.966	99.210	102.190	184.586	232.703	275.121
8			36.840	86.479	95.367	152.089	170.805	194.820	
9			36.817	86.207	95.144	150.563	164.946	191.087	
10			36.796	86.135	95.129	150.159	163.284	190.063	
Wu (2005)			36.774	86.321	95.283	151.126	162.601	—	
0.2		4	28.889	59.679	63.245	98.893	107.491	116.157	
		6	28.035	57.167	61.557	87.426	93.574	103.834	
		7	27.965	56.801	61.423	85.863	92.281	102.064	
		8	27.935	56.751	61.336	84.782	91.021	101.451	
		9	27.925	56.723	61.305	84.483	90.862	101.258	
		10	27.923	56.705	61.298	84.439	90.707	101.192	
Wu (2005)		27.921	56.732	61.325	84.515	90.777	—		

and internal columns, and they are given as follows

$$\begin{aligned}
 U^P = & \frac{1}{2} \int_D \left[\frac{68}{105} \left(\frac{\partial \theta_x}{\partial x} \right)^2 + \frac{68}{105} \left(\frac{\partial \theta_y}{\partial y} \right)^2 + \frac{1}{21} \left(\frac{\partial^2 w}{\partial x^2} \right)^2 + \frac{1}{21} \left(\frac{\partial^2 w}{\partial y^2} \right)^2 \right] dA \\
 & - \frac{1}{2} \int_D \left[\frac{32}{105} \frac{\partial \theta_x}{\partial x} \frac{\partial^2 w}{\partial x^2} + \frac{32}{105} \frac{\partial \theta_y}{\partial y} \frac{\partial^2 w}{\partial y^2} \right] dA \\
 & + \frac{1}{2} \int_D 2\nu D \left[\frac{68}{105} \frac{\partial \theta_x}{\partial x} \frac{\partial \theta_y}{\partial y} + \frac{1}{21} \frac{\partial^2 w}{\partial x^2} \frac{\partial^2 w}{\partial y^2} - \frac{16}{105} \frac{\partial \theta_x}{\partial x} \frac{\partial^2 w}{\partial y^2} - \frac{16}{105} \frac{\partial \theta_y}{\partial y} \frac{\partial^2 w}{\partial x^2} \right] dA
 \end{aligned}$$

$$\begin{aligned}
 & + \frac{1}{2} \int \frac{1-\nu}{2} D \frac{68}{105} \left[\frac{\partial \theta_x}{\partial y} + \frac{\partial \theta_y}{\partial x} \right]^2 dA \\
 & + \frac{1}{2} \int \frac{1-\nu}{2} D \left[\frac{4}{21} \left(\frac{\partial^2 w}{\partial x \partial y} \right)^2 - \frac{64}{105} \frac{\partial^2 w}{\partial x \partial y} \frac{\partial \theta_x}{\partial y} - \frac{64}{105} \frac{\partial^2 w}{\partial x \partial y} \frac{\partial \theta_y}{\partial x} \right] dA \\
 & + \frac{1}{2} \int \frac{8}{15} Gh \left[\left(\theta_x + \frac{\partial w}{\partial x} \right)^2 + \left(\theta_y + \frac{\partial w}{\partial y} \right)^2 \right] dA
 \end{aligned} \tag{4}$$

$$\begin{aligned}
 U^S = & \frac{\delta_1}{2} \int_{AB} k_L w^2 ds + \frac{\delta_2}{2} \int_{BC} k_L w^2 ds + \frac{\delta_3}{2} \int_{CD} k_L w^2 ds + \frac{\delta_4}{2} \int_{DA} k_L w^2 ds \\
 & + \frac{\delta_5}{2} \int_{AB} k_R \theta_n^2 ds + \frac{\delta_6}{2} \int_{BC} k_R \theta_n^2 ds + \frac{\delta_7}{2} \int_{CD} k_R \theta_n^2 ds + \frac{\delta_8}{2} \int_{DA} k_R \theta_n^2 ds \\
 & + \frac{\delta_9}{2} \int_{AB} k_T \theta_s^2 ds + \frac{\delta_{10}}{2} \int_{BC} k_T \theta_s^2 ds + \frac{\delta_{11}}{2} \int_{CD} k_T \theta_s^2 ds + \frac{\delta_{12}}{2} \int_{DA} k_T \theta_s^2 ds
 \end{aligned} \tag{5}$$

where k_L, k_R, k_T are the elastic coefficients of lateral spring, rotational spring and torsional spring respectively; $\delta_i (i = 1, 2, \dots, 12)$ is a governing factor for $\delta_i = 0$ implies the corresponding edge is free while $\delta_i = 1$ the corresponding edge is elastically constrained. For convenience of presentation, the coefficients of the elastic springs are represented in terms of the plate flexural rigidity, i.e., $k_L = \mu_L D/a^3$, $k_R = \mu_R D/a$, $k_T = \mu_T D/a$. θ_n and θ_s are, respectively, the rotations of the mid-plane in the normal plane and in the tangent plane to the plate boundary, and the subscripts n and s represent, respectively, the normal and tangent directions of the edge. These rotations can be obtained by the composition of rotations along x and y directions, and they are expressed as

Table 2 Convergence and comparison of frequency parameters $\lambda = \omega a^2/\pi^2 \sqrt{\rho h/D}$ for a square plate with elastic boundary conditions

h/a	p	Mode sequence number							
		1	2	3	4	5	6	7	8
0.001	7	68.305	193.938	193.938	649.119	740.816	799.786	1082.148	1082.148
	8	3.647	122.096	122.096	171.961	316.773	340.188	878.136	878.136
	9	3.647	7.527	7.527	99.073	211.509	227.620	238.353	238.353
	10	3.647	7.526	7.526	11.002	13.905	14.038	145.428	145.428
	11	3.647	7.440	7.440	11.002	13.897	14.018	17.102	17.102
	Xiang (1997)	3.646	7.437	7.437	10.965	13.332	13.397	16.738	16.737
0.2	7	2.668	4.693	4.693	6.864	8.103	8.379	9.743	9.743
	8	2.666	4.664	4.664	6.280	7.189	7.334	9.412	9.412
	9	2.666	4.654	4.654	6.227	7.153	7.308	8.524	8.524
	10	2.666	4.653	4.653	6.210	7.114	7.267	8.458	8.458
	11	2.666	4.653	4.653	6.210	7.114	7.264	8.411	8.411
	Xiang (1997)	2.639	4.593	4.593	6.123	7.008	7.156	8.280	8.280

$$\theta_n = n_x \theta_x + n_y \theta_y, \quad \theta_s = -n_y \theta_x + n_x \theta_y \quad (6)$$

where n_x and n_y are the cosines of the boundary normal. Substituting Eq. (6) into Eq. (5), one has

$$\begin{aligned} U^S = & \frac{\delta_1}{2} \int_{AB} k_L W^2 ds + \frac{\delta_2}{2} \int_{BC} k_L W^2 ds + \frac{\delta_3}{2} \int_{CD} k_L W^2 ds + \frac{\delta_4}{2} \int_{DA} k_L W^2 ds \\ & + \frac{\delta_5}{2} \int_{AB} k_R (n_{xAB} \theta_x + n_{yAB} \theta_y)^2 ds + \frac{\delta_6}{2} \int_{BC} k_R (n_{xBC} \theta_x + n_{yBC} \theta_y)^2 ds \\ & + \frac{\delta_7}{2} \int_{CD} k_R (n_{xCD} \theta_x + n_{yCD} \theta_y)^2 ds + \frac{\delta_8}{2} \int_{DA} k_R (n_{xDA} \theta_x + n_{yDA} \theta_y)^2 ds \\ & + \frac{\delta_9}{2} \int_{AB} k_T (-n_{yAB} \theta_x + n_{xAB} \theta_y)^2 ds + \frac{\delta_{10}}{2} \int_{BC} k_T (-n_{yBC} \theta_x + n_{xBC} \theta_y)^2 ds \\ & + \frac{\delta_{11}}{2} \int_{CD} k_T (-n_{yCD} \theta_x + n_{xCD} \theta_y)^2 ds + \frac{\delta_{12}}{2} \int_{DA} k_T (-n_{yDA} \theta_x + n_{xDA} \theta_y)^2 ds \end{aligned} \quad (7)$$

The internal columns are simulated as the following two models in this paper

Model A: Point elastic supports in three directions

Since the size of the cross section of the column is much smaller than the dimension of the plate, it can be modeled as three elastic massless springs that restraint the rotations and deflection of the plate. The potential energy of the columns for this model is easily obtained

$$U^C = \frac{1}{2} \sum_{i=1}^n [k_{fi} W^2(x_i, y_i) + k_{xi} \theta_x^2(x_i, y_i) + k_{yi} \theta_y^2(x_i, y_i)] \quad (8)$$

where, k_{fi}, k_{xi}, k_{yi} are the elastic modulus of these springs in lateral and rotational directions. When the column is fixed to the foundation at the other end, they are given by

$$k_{fi} = EA_i/H, \quad k_{xi} = 4EI_y/H, \quad k_{yi} = 4EI_x/H \quad (9a,b,c)$$

where A_i is the area of the cross section; H is the length of the column; I_y and I_x are the second

Table 3 Convergence characteristics of frequency parameters $\lambda = \omega a^2 \sqrt{\rho h/D}$ for a simply supported quadrilateral plate with one inner column support (Model A)

p	Mode sequence number					
	1	2	3	4	5	6
4	26.400	55.301	56.959	108.728	127.430	166.639
6	24.776	51.229	52.211	97.845	108.882	123.667
7	24.553	50.618	51.244	97.391	106.234	114.032
8	24.408	50.466	51.141	97.080	104.732	112.663
9	24.284	50.058	51.000	96.852	103.172	110.693
10	24.227	49.857	50.965	96.752	102.861	110.301

moments of area about the y and x axis respectively. When the column is supported by a pin at the other end, they are given by

$$f_{fi} = EA_i/H, \quad k_{xi} = 3EI_y/H, \quad k_{yi} = 3EI_x/H \quad (10a,b,c)$$

Model B: *Uniformly distributed spring*

The column can also be treated as distributed (or patch) supports only in the longitudinal direction, it is assumed to have only a mean axial stiffness and no rotational stiffness. In this case, the strain energy of the columns is

$$U^C = \frac{1}{2} \sum_{i=1}^n \left(\int_V k_{fi}(x,y) w^2 dA \right) \quad (11)$$

where

$$k_f = E/H \quad (12)$$

The maximum kinetic energy of the plate is

$$T_{\max} = \frac{1}{2} \omega^2 \rho \left\{ hw^2 + \frac{17h^3}{315} (\theta_x^2 + \theta_y^2) + \frac{8h^3}{315} \left(\theta_x \frac{\partial w}{\partial x} + \theta_y \frac{\partial w}{\partial y} \right) + \frac{h^2}{252} \left[\left(\frac{\partial w}{\partial x} \right)^2 + \left(\frac{\partial w}{\partial y} \right)^2 \right] \right\} dA \quad (13)$$

where ρ and ω are, respectively, the mass density and vibrating circular frequency of the plate.

2.3 Coordinate transformation

For convenience of numerical integration and application of boundary conditions, the quadrilateral plate in the $x-y$ plane is mapped onto a basic square domain in the $\xi-\eta$ plane (as shown in Fig. 2(b)) by using the coordinate transformation defined by

$$x = \sum_{i=1}^4 N_i x_i, \quad y = \sum_{i=1}^4 N_i y_i \quad (14)$$

where x_i and y_i are the coordinates of the i th corner of the quadrilateral plate in the $x-y$ plane. The mapping function N_i are defined by

Table 4 Convergence characteristics of frequency parameters $\lambda = \omega a^2 \sqrt{\rho h/D}$ for a quadrilateral plate with two inner column supports and two opposite edges simply supported while the other two opposite edges free (Model A)

p	Mode sequence number					
	1	2	3	4	5	6
4	27.242	57.994	66.397	157.676	159.726	175.445
6	25.860	53.252	58.638	111.984	135.472	145.228
7	25.678	52.144	58.152	108.735	131.949	141.542
8	25.562	51.897	57.457	107.362	129.803	138.673
9	25.497	51.437	57.252	106.790	129.431	136.078
10	25.421	51.280	57.037	106.572	128.752	135.124

Table 5 Comparison study of frequency parameters $\lambda = \omega a^2 \sqrt{\rho h/D}$ for a square plate with four simply supported edges and an internal column at the plate center

Column section	Column model	Mode sequence number					
		1	2	3	4	5	6
0.5 × 0.5	A	49.232	52.475	52.475	78.214	97.901	111.455
	Huang (2001)	49.348	52.401	52.837	78.959	98.711	—
	B	50.688	50.688	57.255	78.218	110.859	127.310
	Huang (2001)	50.858	50.898	59.248	78.968	111.133	—
0.8 × 0.8	A	51.044	54.674	54.674	78.214	97.901	128.824
	Huang (2001)	51.896	54.118	55.279	78.959	98.711	—
	B	56.211	56.992	63.992	78.357	122.948	129.564
	Huang (2001)	55.521	56.089	64.839	79.097	123.032	—
1 × 1	A	54.095	55.351	55.351	78.214	97.901	131.573
	Huang (2001)	52.171	54.421	55.755	78.959	98.711	—
	B	57.266	62.427	65.427	78.762	126.210	131.380
	Huang (2001)	59.312	60.865	67.285	79.423	128.929	—

$$N_i = \frac{1}{4}(1 + \xi\xi_i)(1 + \eta\eta_i) \quad (i = 1, 2, 3, 4) \tag{15}$$

where ξ_i and η_i are the coordinates of the i th corner of the square basic plate in the $\xi - \eta$ plane.

According to the chain rule of differentiation, the first and the second order derivatives of any quantity in the two coordinate systems are related by

$$\begin{Bmatrix} \frac{\partial}{\partial x} \\ \frac{\partial}{\partial y} \end{Bmatrix} = J_1^{-1} \begin{Bmatrix} \frac{\partial}{\partial \xi} \\ \frac{\partial}{\partial \eta} \end{Bmatrix}, \quad \begin{Bmatrix} \frac{\partial^2}{\partial x^2} \\ \frac{\partial^2}{\partial y^2} \\ \frac{\partial^2}{\partial x \partial y} \end{Bmatrix} = J_2^{-1} \begin{Bmatrix} \frac{\partial^2}{\partial \xi^2} \\ \frac{\partial^2}{\partial \eta^2} \\ \frac{\partial^2}{\partial \xi \partial \eta} - \alpha' \frac{\partial}{\partial \xi} + \beta' \frac{\partial}{\partial \eta} \end{Bmatrix} \tag{16}$$

where J_1 and J_2 are, respectively, the first and the second order Jacobian matrices of the geometric mapping, and they are expressed as

$$J_1 = \begin{bmatrix} \frac{\partial x}{\partial \xi} & \frac{\partial y}{\partial \xi} \\ \frac{\partial x}{\partial \eta} & \frac{\partial y}{\partial \eta} \end{bmatrix}, \quad J_2 = \begin{Bmatrix} \left(\frac{\partial x}{\partial \xi}\right)^2 & \left(\frac{\partial y}{\partial \xi}\right)^2 & 2\left(\frac{\partial x}{\partial \xi}\right)\left(\frac{\partial y}{\partial \xi}\right) \\ \left(\frac{\partial x}{\partial \eta}\right)^2 & \left(\frac{\partial y}{\partial \eta}\right)^2 & 2\left(\frac{\partial x}{\partial \eta}\right)\left(\frac{\partial y}{\partial \eta}\right) \\ \left(\frac{\partial x}{\partial \xi}\right)\left(\frac{\partial x}{\partial \eta}\right) & \left(\frac{\partial y}{\partial \xi}\right)\left(\frac{\partial y}{\partial \eta}\right) & \left(\frac{\partial x}{\partial \xi}\right)\left(\frac{\partial y}{\partial \eta}\right) + \left(\frac{\partial y}{\partial \xi}\right)\left(\frac{\partial x}{\partial \eta}\right) \end{Bmatrix} \tag{17}$$

Table 6 Influence of spring stiffness on the frequency parameters $\lambda = \omega a^2 \sqrt{\rho h/D}$ of a quadrilateral plate with elastic boundary conditions and an internal column support at center (Model A)

μ_L	μ_R	μ_T	Mode sequence number					
			1	2	3	4	5	6
10^0	10^8	10^8	5.797	20.147	22.735	40.694	47.641	57.064
10^2	10^8	10^8	32.636	47.256	49.183	65.458	68.661	75.016
10^4	10^8	10^8	42.871	67.649	71.748	93.885	98.646	107.541
10^6	10^8	10^8	43.016	67.985	72.127	94.427	99.281	108.243
10^8	10^8	10^0	42.726	67.409	71.633	93.317	98.601	107.723
10^8	10^8	10^2	43.005	67.967	72.112	94.392	99.258	108.225
10^8	10^8	10^4	43.017	67.988	72.130	94.432	99.287	108.250
10^8	10^8	10^6	43.017	67.989	72.130	94.432	99.288	108.251
10^8	10^8	10^8	43.017	67.989	72.130	94.432	99.288	108.250
10^2	10^0	10^2	28.260	46.371	48.609	65.073	67.421	72.577
10^2	10^2	10^2	32.466	47.178	49.121	65.353	68.567	74.889
10^2	10^4	10^2	32.617	47.213	49.145	65.364	68.601	74.962
10^2	10^6	10^2	32.619	47.214	49.145	65.364	68.601	74.962
10^2	10^8	10^2	32.619	47.214	49.145	65.364	68.601	74.962

The factors α', β' in Eq. (16) are written as

$$\alpha' = \left(\alpha \frac{\partial y}{\partial \eta} - \beta \frac{\partial y}{\partial \xi} \right) / |J_1|, \quad \beta' = \left(\alpha \frac{\partial x}{\partial \eta} - \beta \frac{\partial x}{\partial \xi} \right) / |J_1|$$

where

$$\alpha = \sum_{i=1}^4 \frac{1}{4} \xi_i \eta_i x_i, \quad \beta = \sum_{i=1}^4 \frac{1}{4} \xi_i \eta_i y_i$$

2.4 pb-2 Ritz functions

The admissible functions of deflection and rotations of the plate may be assumed to be a set of pb-2 Ritz functions in the $\xi-\eta$ plane as follows

$$w(\xi, \eta) = \sum_{q=0}^{p_1} \sum_{r=0}^q c_i \phi_i(\xi, \eta) = \sum_{i=1}^m c_i \phi_i(\xi, \eta) = c^T \Phi \tag{18a}$$

$$\theta_x(\xi, \eta) = \sum_{q=0}^{p_2} \sum_{r=0}^q d_i \psi_{xi}(\xi, \eta) = \sum_{i=1}^n d_i \psi_{xi}(\xi, \eta) = d^T \Psi_x \tag{18b}$$

$$\theta_y(\xi, \eta) = \sum_{q=0}^{p_3} \sum_{r=0}^q e_i \psi_{yi}(\xi, \eta) = \sum_{i=1}^l e_i \psi_{yi}(\xi, \eta) = e^T \Psi_y \tag{18c}$$

where p_1, p_2, p_3 are the degrees of the mathematically complete two-dimensional polynomial space; c_i, d_i and e_i are the unknown coefficients to be determined, whose subscript i is given by

$$i = (q+1)(q+2)/2 - (q-r) \quad (19)$$

c, d, e are the unknown coefficient vectors with corresponding elements of c_i, d_i and e_i ; m, n, l are, respectively, the dimensions of c, d, e and given by

$$m = \frac{1}{2}(p_1+1)(p_1+2), \quad n = \frac{1}{2}(p_2+1)(p_2+2), \quad l = \frac{1}{2}(p_3+1)(p_3+2) \quad (20a,b,c)$$

Φ, Ψ_x, Ψ_y are the pb-2 Ritz function vectors whose elements are given as

$$\phi_i = \xi^{q-r} \eta^r \cdot B(\xi, \eta), \quad \psi_{xi} = \xi^{q-r} \eta^r \cdot C(\xi, \eta), \quad \psi_{yi} = \xi^{q-r} \eta^r \cdot D(\xi, \eta) \quad (21)$$

where $B(\xi, \eta), C(\xi, \eta), D(\xi, \eta)$ are, respectively, the basic functions which consist of the products of each boundary expression so as to satisfy the boundary conditions automatically. These basic functions are given as

$$B(\xi, \eta) = (\eta+1)^{S_1} (\xi-1)^{S_2} (\eta-1)^{S_3} (\xi+1)^{S_4} \quad (22a)$$

$$C(\xi, \eta) = (\eta+1)^{S_5} (\xi-1)^{S_6} (\eta-1)^{S_7} (\xi+1)^{S_8} \quad (22b)$$

$$D(\xi, \eta) = (\eta+1)^{S_9} (\xi-1)^{S_{10}} (\eta-1)^{S_{11}} (\xi+1)^{S_{12}} \quad (22c)$$

where S_i depends on the support edge conditions. Takes the edge $y = 0$ ($\eta = -1$) as an example, when the edge is clamped, $S_1 = S_5 = S_9 = 1$; if the edge is simply supported, $S_1 = 1, S_5 = 0, S_9 = 0$; when the edge is free or elastic support, $S_1 = S_5 = S_9 = 0$.

2.5 Eigenvalue problem

By transforming the integration domain of the integrals in Eq. (4), (7), (11) and (13) into $\xi-\eta$ plane and substituting Eq. (18) in the resulting expressions, the energy functional in Eq. (2) can be written as

$$\Pi = \frac{1}{2} q^T (K - \omega^2 M) q \quad (23)$$

in which

$$q^T = [c^T \quad d^T \quad e^T] \quad (24)$$

$$K = K^P + K^S + K^C \quad (25)$$

where K^P, K^S, K^C are, respectively, the stiffness matrices corresponding to plate, springs and columns and M are the mass matrix of the plate. They are given as

$$K^P = \begin{bmatrix} K_{cc}^P & K_{cd}^P & K_{ce}^P \\ & K_{dd}^P & K_{de}^P \\ \text{symmetric} & & K_{ee}^P \end{bmatrix}, \quad K^S = \begin{bmatrix} K_{cc}^S & K_{cd}^S & K_{ce}^S \\ & K_{dd}^S & K_{de}^S \\ \text{symmetric} & & K_{ee}^S \end{bmatrix} \quad (26)$$

$$K^C = \begin{bmatrix} K_{cc}^C & K_{cd}^C & K_{ce}^C \\ & K_{dd}^C & K_{de}^C \\ \text{symmetric} & & K_{ee}^C \end{bmatrix}, \quad M = \begin{bmatrix} M_{cc} & M_{cd} & M_{ce} \\ & M_{dd} & M_{de} \\ \text{symmetric} & & \end{bmatrix}$$

where

$$K_{cc}^P = \int_{-1}^1 \int_{-1}^1 \frac{1}{21} D \left[\frac{\partial^2 \Phi}{\partial x^2} \frac{\partial^2 \Phi^T}{\partial x^2} + \frac{\partial^2 \Phi}{\partial y^2} \frac{\partial^2 \Phi^T}{\partial y^2} \right] |J_1| d\xi d\eta$$

$$+ \int_{-1}^1 \int_{-1}^1 \frac{1}{21} D \left[2\nu \frac{\partial^2 \Phi}{\partial x^2} \frac{\partial^2 \Phi^T}{\partial y^2} + 2(1-\nu) \frac{\partial^2 \Phi}{\partial x \partial y} \frac{\partial^2 \Phi^T}{\partial x \partial y} \right] |J_1| d\xi d\eta \quad (27a)$$

$$+ \int_{-1}^1 \int_{-1}^1 \frac{8}{15} Gh \left[\frac{\partial \Phi}{\partial x} \frac{\partial \Phi^T}{\partial x} + \frac{\partial \Phi}{\partial y} \frac{\partial \Phi^T}{\partial y} \right] |J_1| d\xi d\eta$$

$$K_{dd}^P = \int_{-1}^1 \int_{-1}^1 \left[\frac{68D}{105} \frac{\partial \Psi_x}{\partial x} \frac{\partial \Psi_x^T}{\partial x} + \frac{34(1-\nu)D}{105} \frac{\partial \Psi_x}{\partial y} \frac{\partial \Psi_x^T}{\partial y} + \frac{8}{15} Gh \Psi_x \Psi_x^T \right] |J_1| d\xi d\eta \quad (27b)$$

$$K_{ee}^P = \int_{-1}^1 \int_{-1}^1 \left[\frac{68D}{105} \frac{\partial \Psi_y}{\partial y} \frac{\partial \Psi_y^T}{\partial y} + \frac{34(1-\nu)D}{105} \frac{\partial \Psi_y}{\partial x} \frac{\partial \Psi_y^T}{\partial x} + \frac{8}{15} Gh \Psi_y \Psi_y^T \right] |J_1| d\xi d\eta \quad (27c)$$

$$K_{cd}^P = \int_{-1}^1 \int_{-1}^1 \left[\frac{16D}{105} \frac{\partial^2 \Phi}{\partial x^2} \frac{\partial \Psi_x^T}{\partial x} - \frac{16\nu D}{105} \frac{\partial^2 \Phi}{\partial y^2} \frac{\partial \Psi_x^T}{\partial x} \right] |J_1| d\xi d\eta \quad (27d)$$

$$+ \int_{-1}^1 \int_{-1}^1 \left[-\frac{16(1-\nu)D}{105} \frac{\partial^2 \Phi}{\partial x \partial y} \frac{\partial \Psi_x^T}{\partial y} + \frac{8Gh}{15} \frac{\partial \Phi}{\partial x} \Psi_x^T \right] |J_1| d\xi d\eta$$

$$K_{ce}^P = \int_{-1}^1 \int_{-1}^1 \left[\frac{16D}{105} \frac{\partial^2 \Phi}{\partial y^2} \frac{\partial \Psi_y^T}{\partial y} - \frac{16\nu D}{105} \frac{\partial^2 \Phi}{\partial x^2} \frac{\partial \Psi_y^T}{\partial y} \right] |J_1| d\xi d\eta \quad (27e)$$

$$+ \int_{-1}^1 \int_{-1}^1 \left[-\frac{16(1-\nu)D}{105} \frac{\partial^2 \Phi}{\partial x \partial y} \frac{\partial \Psi_y^T}{\partial x} + \frac{8Gh}{15} \frac{\partial \Phi}{\partial y} \Psi_y^T \right] |J_1| d\xi d\eta$$

$$K_{de}^P = \int_{-1}^1 \int_{-1}^1 \left[\frac{68\nu D}{105} \frac{\partial \Psi_x}{\partial x} \frac{\partial \Psi_y^T}{\partial y} + \frac{34(1-\nu)D}{105} \frac{\partial \Psi_x}{\partial y} \frac{\partial \Psi_y^T}{\partial x} \right] |J_1| d\xi d\eta \quad (27f)$$

$$K_{cc}^S = \int_{-1}^1 k_L \delta_1 [\Phi \Phi^T] \Big|_{\eta=-1} L_{AB} d\xi + \int_{-1}^1 k_L \delta_2 [\Phi \Phi^T] \Big|_{\xi=1} L_{BC} d\eta \quad (28a)$$

$$+ \int_{-1}^1 k_L \delta_3 [\Phi \Phi^T] \Big|_{\eta=1} L_{CD} d\xi + \int_{-1}^1 k_L \delta_4 [\Phi \Phi^T] \Big|_{\xi=-1} L_{DA} d\eta$$

$$\begin{aligned}
K_{dd}^S &= \int_{-1}^1 k_R \delta_5 n_{xAB}^2 [\Psi_x \Psi_x^T]_{\eta=-1} L_{AB} d\xi + \int_{-1}^1 k_R \delta_6 n_{xBC}^2 [\Psi_x \Psi_x^T]_{\xi=1} L_{BC} d\eta \\
&+ \int_{-1}^1 k_R \delta_7 n_{xCD}^2 [\Psi_x \Psi_x^T]_{\eta=1} L_{CD} d\xi + \int_{-1}^1 k_R \delta_8 n_{xDA}^2 [\Psi_x \Psi_x^T]_{\xi=-1} L_{DA} d\eta \\
&+ \int_{-1}^1 k_T \delta_9 n_{yAB}^2 [\Psi_y \Psi_y^T]_{\eta=-1} L_{AB} d\xi + \int_{-1}^1 k_T \delta_{10} n_{yBC}^2 [\Psi_y \Psi_y^T]_{\xi=1} L_{BC} d\eta \\
&+ \int_{-1}^1 k_T \delta_{11} n_{yCD}^2 [\Psi_y \Psi_y^T]_{\eta=1} L_{CD} d\xi + \int_{-1}^1 k_T \delta_{12} n_{yDA}^2 [\Psi_y \Psi_y^T]_{\xi=-1} L_{DA} d\eta
\end{aligned} \tag{28b}$$

$$\begin{aligned}
K_{ee}^S &= \int_{-1}^1 k_R \delta_5 n_{yAB}^2 [\Psi_y \Psi_y^T]_{\eta=-1} L_{AB} d\xi + \int_{-1}^1 k_R \delta_6 n_{yBC}^2 [\Psi_y \Psi_y^T]_{\xi=1} L_{BC} d\eta \\
&+ \int_{-1}^1 k_R \delta_7 n_{yCD}^2 [\Psi_y \Psi_y^T]_{\eta=1} L_{CD} d\xi + \int_{-1}^1 k_R \delta_8 n_{yDA}^2 [\Psi_y \Psi_y^T]_{\xi=-1} L_{DA} d\eta \\
&+ \int_{-1}^1 k_T \delta_9 n_{xAB}^2 [\Psi_x \Psi_x^T]_{\eta=-1} L_{AB} d\xi + \int_{-1}^1 k_T \delta_{10} n_{xBC}^2 [\Psi_x \Psi_x^T]_{\xi=1} L_{BC} d\eta \\
&+ \int_{-1}^1 k_T \delta_{11} n_{xCD}^2 [\Psi_x \Psi_x^T]_{\eta=1} L_{CD} d\xi + \int_{-1}^1 k_T \delta_{12} n_{xDA}^2 [\Psi_x \Psi_x^T]_{\xi=-1} L_{DA} d\eta
\end{aligned} \tag{28c}$$

$$K_{cd}^S = K_{ce}^S = 0 \tag{28d}$$

$$\begin{aligned}
K_{de}^S &= \int_{-1}^1 k_R \delta_5 n_{xAB} n_{yAB} [\Psi_x \Psi_y^T]_{\eta=-1} L_{AB} d\xi + \int_{-1}^1 k_R \delta_6 n_{xBC} n_{yBC} [\Psi_x \Psi_y^T]_{\xi=1} L_{BC} d\eta \\
&+ \int_{-1}^1 k_R \delta_7 n_{xCD} n_{yCD} [\Psi_x \Psi_y^T]_{\eta=1} L_{CD} d\xi + \int_{-1}^1 k_R \delta_8 n_{xDA} n_{yDA} [\Psi_x \Psi_y^T]_{\xi=-1} L_{DA} d\eta \\
&- \int_{-1}^1 k_T \delta_9 n_{xAB} n_{yAB} [\Psi_x \Psi_y^T]_{\eta=-1} L_{AB} d\xi - \int_{-1}^1 k_T \delta_{10} n_{xBC} n_{yBC} [\Psi_x \Psi_y^T]_{\xi=1} L_{BC} d\eta \\
&- \int_{-1}^1 k_T \delta_{11} n_{xCD} n_{yCD} [\Psi_x \Psi_y^T]_{\eta=1} L_{CD} d\xi - \int_{-1}^1 k_T \delta_{12} n_{xDA} n_{yDA} [\Psi_x \Psi_y^T]_{\xi=-1} L_{DA} d\eta
\end{aligned} \tag{28e}$$

$$K_{cc}^C = \sum_{i=1}^n k_{fi} [\Phi(\xi_i, \eta_i)] [\Phi(\xi_i, \eta_i)]^T \quad \text{or} \quad K_{cc}^C = \sum_{i=1}^n \frac{ab}{4} \int_{\xi_0}^{\xi_i} \int_{\eta_0}^{\eta_i} k_{fi} \Phi \Phi^T d\xi d\eta \tag{29a}$$

$$K_{dd}^C = \sum_{i=1}^n k_{xi} [\Psi_x(\xi_i, \eta_i)] [\Psi_x(\xi_i, \eta_i)]^T \quad \text{or} \quad K_{dd}^C = 0 \tag{29b}$$

$$K_{ee}^C = \sum_{i=1}^n k_{yi} [\Psi_y(\xi_i, \eta_i)] [\Psi_y(\xi_i, \eta_i)]^T \quad \text{or} \quad K_{ee}^C = 0 \tag{29c}$$

$$K_{cd}^C = K_{ce}^C = K_{de}^C = 0 \tag{29d}$$

$$M_{cc} = \int_{-1}^1 \int_{-1}^1 \left[\rho h \Phi \Phi^T + \frac{\rho h^3}{252} \left(\frac{\partial \Phi}{\partial x} \frac{\partial \Phi^T}{\partial x} + \frac{\partial \Phi}{\partial y} \frac{\partial \Phi^T}{\partial y} \right) \right] |J_1| d\xi d\eta, \quad M_{de} = 0 \tag{30a,b}$$

Table 7 Comparison of frequency parameters $\lambda = \omega a^2 \sqrt{\rho h/D}$ for a quadrilateral plate having center column support between two kinds of column models

μ_L	μ_R	μ_T	Column Model	Mode sequence number					
				1	2	3	4	5	6
0	0	0	A	0.842	0.876	3.491	20.505	25.560	33.282
			B	0.842	0.898	6.622	20.507	25.799	33.749
10^8	0	0	A	28.721	56.730	61.333	84.459	91.008	101.373
			B	30.812	56.785	61.414	84.475	91.420	101.707
10^8	10^8	10^8	A	43.017	68.017	72.161	94.435	99.289	108.251
			B	44.877	68.077	72.247	94.451	99.622	108.594

$$M_{dd} = \frac{17\rho h^3}{315} \int_{-1}^1 \int_{-1}^1 [\Psi_x \Psi_x^T] |J_1| d\xi d\eta, \quad M_{ee} = \frac{17\rho h^3}{315} \int_{-1}^1 \int_{-1}^1 [\Psi_y \Psi_y^T] |J_1| d\xi d\eta \quad (30c,d)$$

$$M_{cd} = \frac{4\rho h^3}{315} \int_{-1}^1 \int_{-1}^1 \left[\frac{\partial \Phi}{\partial x} \Psi_x^T \right] |J_1| d\xi d\eta, \quad M_{ce} = \frac{4\rho h^3}{315} \int_{-1}^1 \int_{-1}^1 \left[\frac{\partial \Phi}{\partial y} \Psi_y^T \right] |J_1| d\xi d\eta \quad (30e,f)$$

Setting the first variation of the functional in Eq. (23) to be zero, results in the following eigenvalue equation

$$(K - \omega^2 M)q = 0 \quad (31)$$

In the numerical analysis, Gauss quadrature is employed to evaluate the integrals appearing in Eqs. (27) to (30). Standard eigenvalue solvers can be used to compute the natural frequencies of the plate by solving the general eigenvalue problem defined by Eq. (31).

3. Convergence and comparison studies

In this section, convergency and comparison studies are conducted firstly in order to validate the present numerical method. Firstly, take a quadrilateral plate with classical CCCC and SSSS boundary conditions as an example. The shape of the plate is described in Fig. 2, and the size is assumed $b = 0.8a$, $c = 0.7a$, $\alpha = 70^\circ$, $\beta = 75^\circ$. For convenience of presentation, a non-dimensional frequency parameter $\lambda = \omega a^2 \sqrt{\rho h/D}$ is introduced in this example. The first six natural frequency factors of this plate are computed using the standard eigenvalue solver in Matlab internal matrix function, and the numerical results are presented in Table 1. Both thin and thick plates are considered in this study. From Table 1, it is seen that with increasing the polynomial power p , the frequency parameter λ converges rapidly and monotonically from above to stable values for both thin and thick plate. The convergence rate for thin plate is relatively slower than that for thick plate. We can easily find that for moderately thick plate, the frequency parameter converges very fast even for the higher modes, whether for the simply supported boundary condition or for the fully clamped boundary condition. The corresponding results given by Wu *et al.* (2005) using the differential

cubature method, are also presented in Table 1. It is observed that the present results agree very well with those available in the reference, especially for moderately thick plates.

In the following example, a square plate with for edges elastically supported is considered. The coefficients of the spring stiffness are set as $\mu_L = \mu_R = 10^8$, $\mu_T = 0$. In this study, the frequency parameter is defined as $\lambda = \omega a^2 / \pi^2 \sqrt{\rho h / D}$ in order to compare the present results with those given by other researchers. The first eight frequency parameters are computed and tabulated in Table 2. It is found that whether for thin and thick plate the frequency parameters $\lambda = \omega a^2 / \pi^2 \sqrt{\rho h / D}$ converges monotonically from above to stable values; however, the convergence rate demonstrates different characteristics. For moderately thick plate with $h/a = 0.2$, the convergence rate is very fast. In this case the frequency parameters would have sufficient numerical accuracy just by taking the polynomial index $p = 8$ for the first six modes. However, for thin plate with $h/a = 0.001$, the convergence rate is relatively slow. It is seen that the polynomial index p must be taken as 10 at least so as to obtain results with acceptable accuracy for the first six modes. The present results are also compared to existing results given by Xiang *et al.* (1997). Close agreement is also found in this example.

To further demonstrate the numerical convergency and accuracy of this method for vibration analysis of quadrilateral plates with inner column support, the third example is selected as a quadrilateral thin plate one or two inner column supports. In this case, $a = 10$, $b = 8$, $c = 7$, $\alpha = 70^\circ$, $\beta = 75^\circ$, $h = 0.2$, $\lambda = \omega a^2 \sqrt{\rho h / D}$. The columns of 6 m lengths are fixed to the foundation. Model A is employed in the computation. Table 3 is the numerical results of the frequency parameters for plate with inner one column at the plate center and four edges simply support conditions. The column is with $1 \text{ m} \times 1 \text{ m}$ cross section and located at the cross point of two diagonal straight lines. Table 4 presents the numerical results of the frequency parameters for plate with inner two column supports and two edges simply supported (AC and BD) and the other two edges (AB and CD) free. The two columns are with $0.5 \text{ m} \times 0.5 \text{ m}$ cross sections and the supporting location coordinates are (3.943,3.633) and (6.519,3.507). From these two tables it is observed again that the frequency parameters are converged monotonically from above to stable values, whether for SSSS or SFSE boundary conditions, with one or two internal column supports.

Table 5 is a comparison study of frequency parameters for a square plate with four edges simply supported and an internal column at the center. The relative thickness of the plate is taken as $h/a = 0.02$. We should note that the column models A and B in the present paper are corresponding to models B and C in the reference of Huang (2001). We can see that for almost all cases the present results are close agreement with those given by Huang (2001) except for the large column cross section 1×1 .

It is necessary to point out that the selected order of the polynomial should not be too large, otherwise, the computation would be unstable because the eigen matrix of the problem will be ill-conditioned. For most cases in this section, rational solutions with acceptable numerical accuracies could be obtained when the order of the polynomial p is set as 10. In the following studies, the index p is all chosen as 10 except special statement.

4. Results and discussion

Based on the previous convergence and comparison studies, some new numerical results are presented in this section to study the effects of various factors on the natural frequency parameters.

Firstly, a quadrilateral plate with a column support at center and four edges elastically supported by springs in three directions. In this case, the dimension of the plate is $a = 10$, $b = 8$, $c = 7$, $\alpha = 70^\circ$, $\beta = 75^\circ$, $h = 0.2$. The length and cross section of the column are assumed to be 5 and 1×1 . Poisson's ratio is set as 0.3. The first six frequency parameters $\lambda = \omega a^2 \sqrt{\rho h/D}$ of this plate column system are computed and listed in Table 6. It is found from table 6 that the frequency parameters increase with increasing the relative stiffness of spring. When the relative stiffness of the rotational and torsional springs remains constant, the frequency parameters increase significantly with increasing the relative stiffness of lateral spring. However, this variation trend is not remarkable when the stiffness factor μ_L of lateral spring remains constant. This indicates that the lateral support will have greater influences on the vibration behavior than the rotational support and torsional support.

Table 7 is a comparison of frequency parameters of this plate column system between the two column models. All the factors of this plate are taken the same as the above example. The length and cross section of the column are 5 and 1×1 respectively. It is seen that the difference of the numerical values of frequency parameters between the two column models is very small except some special cases. In general, the numerical values generated by model B are slightly larger than those generated by model A. For the third frequency when the plate is free at four edges and the fundamental frequency when the plate is simply supported at four edges, model B generates much greater numerical values than model A.

Table 8 presents the effect of connecting pattern between the column and the foundation on the frequency parameters of a quadrilateral plate with a center column and elastic edge supports. The plate model is the same as the former cases. The dimensions and location of the column are also taken the same as above. The numerical results are calculated by using column model A. It is obvious that the numerical results generated by fixed mode are slightly larger than those generated by pinned mode. However, the differences of the numerical values between the two different connecting patterns are so small that they can be neglected in engineering.

Table 8 Effects of connecting pattern between column and foundation on the frequency parameters $\lambda = \omega a^2 \sqrt{\rho h/D}$ of a quadrilateral plate having center column and elastic boundary conditions (Model A)

μ_L	μ_R	μ_T	Connection pattern	Mode sequence number					
				1	2	3	4	5	6
0	0	0	Fixed	0.842	0.942	3.491	20.505	25.560	33.282
			pinned	0.730	0.817	3.490	20.503	25.559	33.281
0	10^0	10^0	Fixed	3.445	11.836	13.437	28.702	34.923	42.306
			pinned	3.445	11.828	13.428	28.701	34.922	42.305
0	10^2	10^2	Fixed	3.457	19.212	21.893	39.928	46.974	56.401
			pinned	3.457	19.207	21.886	39.926	46.973	56.401
10^2	0	0	Fixed	24.311	43.429	46.168	60.694	63.274	69.176
			pinned	24.311	43.424	46.162	60.694	63.274	69.176
10^8	10^8	10^8	Fixed	43.017	68.017	72.161	94.435	99.289	108.251
			pinned	43.017	68.010	72.153	94.435	99.289	108.251

Table 9 Frequency parameters $\lambda = \omega a^2 \sqrt{\rho h/D}$ of a quadrilateral thick plate under various column supports and different boundary conditions (Model A)

Boundary conditions	Column location	Mode sequence number					
		1	2	3	4	5	6
<i>EEEE</i> $\mu_L = \mu_R = \mu_T = 0$	Fig. 3(a)	0.242	0.973	3.355	20.691	25.565	33.205
	Fig. 3(b)	0.208	1.067	3.363	20.636	25.605	33.218
	Fig. 3(c)	0.804	2.927	6.867	20.530	26.229	33.693
	Fig. 3(d)	0.909	4.863	5.713	20.955	26.000	33.453
	Fig. 3(e)	4.414	6.707	6.958	20.727	26.947	34.016
	Fig. 3(f)	1.210	3.273	3.543	20.836	25.703	33.312
<i>EEEE</i> $\mu_L = \mu_R = \mu_T = 1$	Fig. 3(a)	4.678	13.387	14.801	29.586	35.433	42.672
	Fig. 3(b)	4.674	13.338	14.860	29.560	35.445	42.687
	Fig. 3(c)	5.466	13.257	15.978	29.507	35.853	43.093
	Fig. 3(d)	6.138	13.960	15.313	29.876	35.627	42.959
	Fig. 3(e)	6.354	14.602	15.993	29.587	36.198	43.386
	Fig. 3(f)	4.752	13.500	14.967	29.652	35.485	42.711
<i>EEEE</i> $\mu_L = \mu_R = \mu_T = 10^4$	Fig. 3(a)	42.172	67.648	71.737	93.950	98.565	107.434
	Fig. 3(b)	42.172	67.647	71.738	93.898	98.557	107.407
	Fig. 3(c)	42.183	67.651	71.775	93.890	98.511	107.454
	Fig. 3(d)	42.263	67.718	71.890	94.112	98.538	107.502
	Fig. 3(e)	42.193	67.691	71.780	93.902	98.570	107.460
	Fig. 3(f)	42.174	67.650	71.742	93.968	98.619	107.439
SSSS	Fig. 3(a)	27.928	56.707	61.301	84.454	90.716	101.202
	Fig. 3(b)	27.927	56.706	61.301	84.443	90.715	101.197
	Fig. 3(c)	27.970	56.724	61.341	84.476	90.719	101.218
	Fig. 3(d)	28.527	56.936	61.981	85.375	90.724	101.476
	Fig. 3(e)	28.012	56.773	61.355	84.516	90.745	101.230
	Fig. 3(f)	27.932	56.707	61.305	84.458	90.724	101.207
CCCC	Fig. 3(a)	42.316	67.979	72.116	94.342	98.867	108.023
	Fig. 3(b)	42.316	67.979	72.116	94.339	98.868	108.024
	Fig. 3(c)	42.321	67.979	72.124	94.340	98.870	108.036
	Fig. 3(d)	42.619	68.160	72.659	95.117	98.877	108.362
	Fig. 3(e)	42.326	67.989	72.125	94.344	98.883	108.037
	Fig. 3(f)	42.317	67.980	72.117	94.344	98.869	108.025

In the following, a quadrilateral plate with two or four internal columns at the side of the plate is analyzed to discuss the influences of the column locations on the frequency parameters. The plate dimensions are also taken as $a = 10$, $b = 8$, $c = 7$, $\alpha = 70^\circ$, $\beta = 75^\circ$, $h = 2$. The height and the area of cross section of the columns are 5 and 1×1 , respectively. Poisson's ratio is also taken to be 0.3. Fig. 3 gives the distributing pattern in various locations of these columns. These columns are located at either the opposite corners or the middle points of the opposite edges of the plate. Table 9

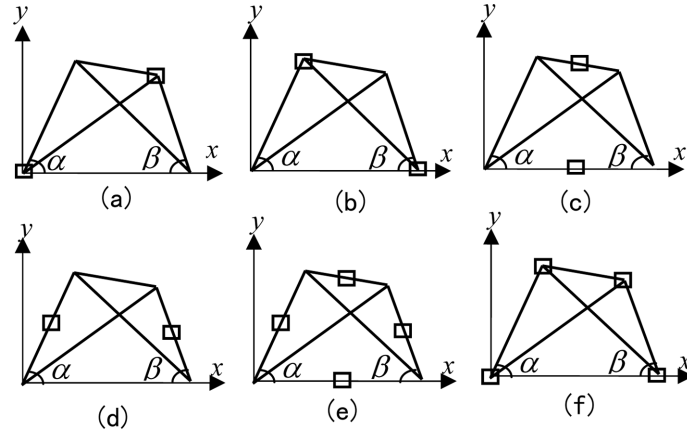


Fig. 3 Arrangement of columns at the edges of the plate

presents the numerical results of the first six natural frequency parameters $\lambda = \omega a^2 \sqrt{\rho h/D}$ for this plate column system. All the numerical results are generated by using Model A for the columns in this problem. Different boundary conditions are considered. It is found from this table that for plates having two columns, Figs. 3(c) and 3(d) generate larger frequency parameters than Figs. 3(a) and 3(b), for the lower modes. This indicates that the columns give much stronger stiffness for the plate when they are arranged at the middle of the edges than at the opposite corner points. For the higher modes however, the frequency parameters keep almost the same values. This implies that the positions of the columns have little effects on the higher mode frequency parameters. It is interesting to find that for the first two modes, Fig. 3(c) generates lower frequency parameters than Fig. 3(d), for the third mode however, the opposite phenomenon occurs, when the stiffness of the elastic springs at the edges of the plate are relatively small. We can also find that the larger the edge spring stiffness, the smaller the effects of the columns location on the frequency parameters will be. When the stiffness factors of spring are taken as $\mu_L = \mu_R = \mu_T = 10$, the numerical results are almost identical to those of the plate with fully clamped boundary conditions (CCCC). For plates with four columns, Fig. 3(e) generates larger frequency parameters than Fig. 3(f) especially for the

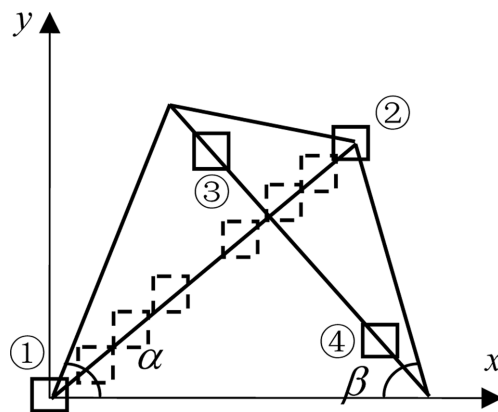


Fig. 4 Arrangement of columns inside the plate

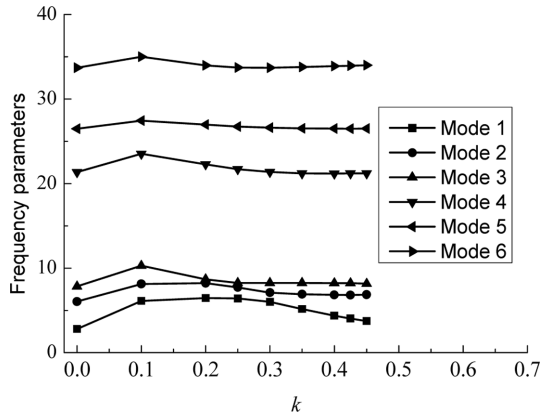


Fig. 5 Frequency parameters vs column location factor ($\mu_L = \mu_R = \mu_T = 0$)

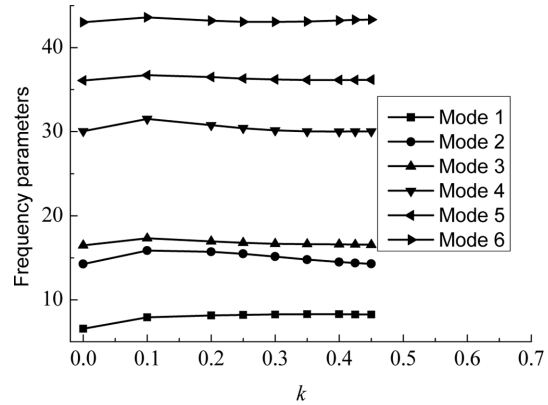


Fig. 6 Frequency parameters vs column location factor ($\mu_L = \mu_R = \mu_T = 1$)

lower modes. When the edge spring stiffness factors becomes large, the numerical results generated by Fig. 3(e) are closed to those generated by Fig. 3(f).

To further study the effects of column locations on the normalized natural frequencies, we set four columns inside the domain of the plate as shown in Fig. 4. Let two columns be located at two fixed points along one diagonal of the plate, while the other two columns are in different positions along the other diagonal of the plate. For convenience of presentation, we define a new variable k , which is the ratio of the distance between a column and the corner nearby to the length of that diagonal. For the two columns ③ and ④ which are located at fixed position, this factor is taken as $k = 0.2$. For columns ① and ② on the other diagonal, variable k changes from 0 to 0.45. All the material constants and dimensional parameters of the plate and the columns are the same as above examples. Also, model A for the columns is used again in this example. Figs. 5 to 9 illustrate the changing tendency of the first six orders frequency parameters $\lambda = \omega a^2 \sqrt{\rho h / D}$ with respect to column location factor k for the plate column system having different boundary conditions. Fig. 5 is the curve of frequency parameters λ vs the column location factor k for a plate with free boundary conditions. From Fig. 5 it is observed that the frequency parameters λ of the plate first increase then decrease with increasing the factor k , and they will have a maximum as k approaches to 0.1, whether for the lower modes or the higher modes. Fig. 6 is the curve of frequency parameters vs factor k for a plate having weak elastic boundary conditions, in which the spring stiffness factors are set as $\mu_L = \mu_R = \mu_T = 1$. Similar phenomenon can be found from this figure. The dimensionless frequency parameters are increased first to a maximum value when k reaches 0.1, then decreased slowly. For the first order mode however, the frequency parameter does not decreased when the factor k across 0.1, it will remain almost a constant value as the column location factor is changed from 0.1 to 0.45. Fig. 7 presents the variation tendency of frequency parameters vs the column location factor k for a plate having strong elastic boundary conditions, in which the spring stiffness factors are set as $\mu_L = \mu_R = \mu_T = 10000$. It is seen that all the frequency parameters change very slowly when the column location factor k is changed from 0 to 0.45. This is due to the strong boundary conditions. For the first three order modes, the frequency parameters would reach unclear maximum values as the factor k is close to 0.3. Figs. 8 and 9 are the curves of frequency parameters vs column location factor k for a plate having simply supported and fully clamped boundary

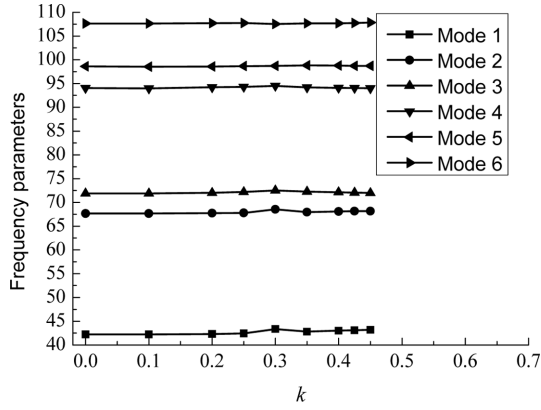


Fig. 7 Frequency parameters vs column location factor ($\mu_L = \mu_R = \mu_T = 10000$)

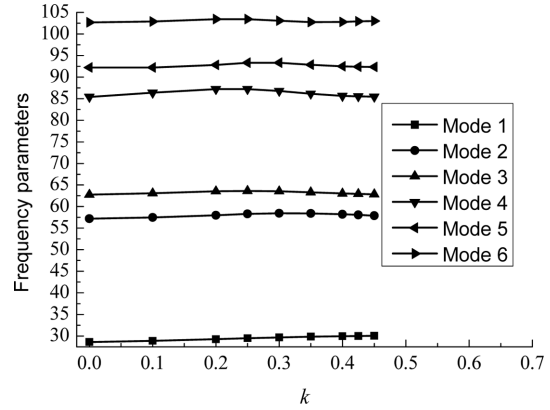


Fig. 8 Frequency parameters vs column location factor (SSSS boundary conditions)

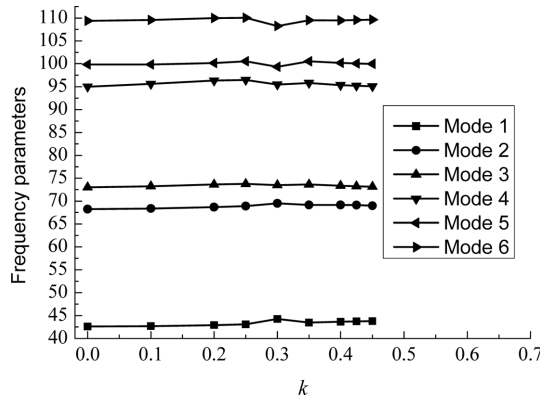


Fig. 9 Frequency parameters vs column location factor (CCCC boundary conditions, Model A)

conditions, respectively. From these two figures one can easily find that the frequency parameters change very slowly with changing the column location along the diagonal of the plate. This is chiefly because the restraint stiffness of the columns is smaller than that of the boundary constraint. It is interesting to find that for case of fully clamped boundary conditions, the two lower order frequency parameters have maximum values, whereas the two higher order frequency parameters have minimum values when the column location factor reaches 0.3.

5. Conclusions

The natural frequencies for arbitrary quadrilateral thick plates with internal column supports and elastic boundary conditions have been investigated by using the powerful pb-2 Ritz energy method combined with Reddy's higher shear deformation theory. Large amount of numerical examples demonstrate the applicability and versatility of the present method through the convergency and comparison studies. Parametric studies on the dimensionless frequencies show:

- (1) The stiffness of lateral spring at the edges of the plate has greater influence on the vibration behavior than the rotational and torsional springs.
- (2) Except some special cases, the differences of the numerical values of frequency parameters between the two column models (elastic point support in three directions and the uniformly distributed springs) are very small.
- (3) The differences of the numerical values of frequency parameters between the two different connecting patterns of column to foundation are small enough to be neglected in engineering.
- (4) When the columns change their position along the edges of the plate, the column locations have significant effects on the lower order frequency parameters, but little effects on the higher order frequency parameters. The columns offer much stronger stiffness for the plate when they are arranged at the middle of the edges than at the corner points.
- (5) When the columns change their position along the diagonal of the plate, the frequency parameters first increase to a maximum then decrease with increasing the column location factor, for plates having weak boundary conditions.

References

- Cheung, Y.K. and Zhou, D. (1999), "The free vibration of rectangular composite plates with point supports using static beam functions", *Compos. Struct.*, **44**, 145-154.
- Cheung, Y.K. and Zhou, D. (2000), "Vibrations of rectangular plates with elastic intermediate line-supports and edge constraints", *Thin Wall. Struct.*, **37**, 305-331.
- Du, J., Li, W.L., Liu, Z., Yang, T. and Jin, G. (2011), "Free vibration of two elastically coupled rectangular plates with uniform elastic boundary restraints", *J. Sound Vib.*, **330**(4), 788-804.
- Fan, S.C. and Cheung, Y.K. (1984), "Flexural free vibrations of rectangular plates with complex support conditions", *J. Sound Vib.*, **93**, 81-94.
- Gorman, D.J. (1999), "Accurate free vibration analysis of point supported Mindlin plates by the superposition method", *J. Sound Vib.*, **219**, 265-277.
- Huang, M.H. and Thambiratnam, D.P. (2001), "Free vibration analysis of rectangular plates on elastic intermediate supports", *J. Sound Vib.*, **240**, 567-580.
- Huang, M.H. and Zhao, M.Y. (2001), "Static and free vibration analysis of plate on column supports by different models", *J. Nanchang Univ.*, **23**(3), 18-25. (in Chinese)
- Karunasena, W., Liew, K.M. and Bermani, F.G.A. (1996), "Natural frequencies of thick arbitrary quadrilateral plates using the pb-2 Ritz method", *J. Sound Vib.*, **196**, 371-385.
- Kim, C.S. and Dickinson, S.M. (1987), "The flexural vibration of rectangular plates with point supports", *J. Sound Vib.*, **117**, 249-261.
- Kitipornchai, S., Xiang, Y. and Liew, K.M. (1994), "Vibration analysis of corner supported Mindlin plates of arbitrary shape using the Lagrange multiplier method", *J. Sound Vib.*, **173**(4), 457-470.
- Lee, L.T. and Lee, D.C. (1997), "Free vibration of rectangular plates on elastic point supports with the application of a new type of admissible function", *Comput. Struct.*, **65**, 149-156.
- Liew, K.M., Xiang, Y., Kitipornchai, S. and Lim, M.K. (1994), "Vibration of Mindlin plates in point supports using constraint functions", *J. Eng. Mech.*, **120**, 499-513.
- Malekzadeh, P. and Karami, G. (2008), "Large amplitude flexural vibration analysis of tapered plates with edges elastically restrained against rotation using DQM", *Eng. Struct.*, **30**, 2850-2858.
- Narita, Y. (1981), "Application of a series-type method to vibration of orthotropic rectangular plates with mixed boundary conditions", *J. Sound Vib.*, **77**, 345-355.
- Narita, Y. (1984), "Note on vibrations of point supported rectangular plates", *J. Sound Vib.*, **93**, 593-597.
- Narita, Y. (1985), "The effects of point constraints on transverse vibration of cantilever plates", *J. Sound Vib.*, **102**, 305-313.

- Ohya, F., Ueda, M., Uchiyama, T. and Kikuchi, M. (2006), "Free vibration analysis by the superposition method of rectangular Mindlin plates with internal columns resting on uniform elastic edge supports", *J. Sound Vib.*, **289**, 1-24.
- Reddy, J.N. (1999), *Theory and Analysis of Elastic Plates*, Taylor & Francis, Philadelphia.
- Seyedemad, M., Massood, M. and John, E.A. (2012), "On the free vibration response of rectangular plates, partially supported on elastic foundation" *Appl. Math. Model.*, **36**, 4473-4482.
- Shufrin, I. and Eisenberger, M. (2005), "Stability and vibration of shear deformable plates—first order and higher order analyses", *Int. J. Solids Struct.*, **42**, 1225-1251.
- Wang, Y., Wang, Z.M. and Ruan, M. (2010), "Application of meshless method in the transverse vibration of rectangular thin plate with elastic point supports", *Chinese J. Comput. Mech.*, **27**(2), 238-243. (in Chinese)
- Wu, L.H. (2001), "Free vibration of arbitrary quadrilateral thick plates", *Chin. Quart. Mech.*, **22**(2), 258-263.
- Wu, L.H. and Liu, J. (2005), "Free vibration analysis of arbitrary shaped thick plates by differential cubature method", *Int. J. Mech. Sci.*, **47**, 63-81.
- Wu, L.H. and Lu, Y. (2011), "Free vibration analysis of rectangular plates with internal columns and uniform elastic edge supports by pb-2 Ritz method", *Int. J. Mech. Sci.*, **53**, 494-504.
- Xiang, Y., Liew, K.M. and Kitipornchai, S. (1997), "Vibration analysis of rectangular plates resting on elastic edge supports", *J. Sound Vib.*, **204**(1), 1-16.
- Zhou, D. (2002), "Vibrations of point supported rectangular plates with variable thickness using a set of static tapered beam functions", *Int. J. Mech. Sci.*, **44**, 149-164.
- Zhou, D. and Ji, T. (2006), "Free vibration of rectangular plates with internal column supports", *J. Sound Vib.*, **297**, 146-166.
- Zhou, D., Cheung, Y.K. and Kong, J. (2000), "Free vibration of thick layered rectangular plates with point supports by finite layer method", *Int. J. Solids Struct.*, **37**, 1483-1499.
- Zhou, D. (2001), "Vibrations of Mindlin rectangular plates with elastic restrained edges using static Timoshenko beam functions in Rayleigh-Ritz method", *Int. J. Solids Struct.*, **38**, 5565-5580.
- Zhou, D., Lo, S.H., Au, F.T.K., Cheung, Y.K. and Liu, W.Q. (2006), "3-D vibration analysis of skew thick plates using Chebyshev-Ritz method", *Int. J. Mech. Sci.*, **48**, 1481-1493.
- Zhou, D., Cheung, Y.K., Au, F.T.K. and Lo, S.H. (2002), "Three-dimensional vibration analysis of thick rectangular plates using Chebyshev polynomial and Ritz method", *Int. J. Solids Struct.*, **39**, 6339-6353.
- Zhou, D., Cheung, Y.K., Lo, S.H. and Au, F.T.K. (2005), "3-D vibration analysis of rectangular plates with mixed boundary conditions", *ASME J. Appl. Mech.*, **72**, 227-236.